Science Advances
AAAS

advances.sciencemag.org/cgi/content/full/4/11/eaat7387/DC1

Supplementary Materials for

Stretchable organic optoelectronic sensorimotor synapse

Yeongjun Lee, Jin Young Oh, Wentao Xu, Onnuri Kim, Taeho Roy Kim, Jiheong Kang, Yeongin Kim, Donghee Son, Jeffery B.-H. Tok, Moon Jeong Park, Zhenan Bao*, Tae-Woo Lee*

*Corresponding author. Email: twlees@snu.ac.kr (T.-W.L.); zbao@stanford.edu (Z.B.)

Published 23 November 2018, *Sci. Adv.* **4**, eaat7387 (2018)
DOI: 10.1126/sciadv.aat7387

The PDF file includes:

Other Supplementary Material for this manuscript includes the following:

(available at advances.sciencemag.org/cgi/content/full/4/11/eaat7387/DC1)

Additional supporting information

Neuromuscular junction and stretchable organic nanowire synaptic transistor (s-ONWST)

A neuromuscular system is composed of a lower motor neuron and skeletal muscle fibers; it enables contraction of skeletal muscles. At a neuromuscular junction between a motor neuron and a muscle fiber, an action potential reaches an axon terminal which is a presynaptic membrane that releases the neurotransmitter acetylcholine through a chemical synapse. Acetylcholine binds to a receptor on a postsynaptic membrane of a muscle cell, and stimulates opening of relevant ion channels that allow ions to flow across the membrane of the muscle tissue. This depolarization of muscle fiber generates a postsynaptic potential that results in muscle contraction. Acetylcholine is the only neurotransmitter in the neuromuscular junction, so only excitatory postsynaptic potential (EPSP) activates muscle contraction.

In our neuromuscular electronic system, s-ONWST emulates the motor neuron and the neuromuscular junction. A buckled ONW has similar morphology to the biological neuron, which has a thin and flexible axon. The gate mimics the presynaptic membrane and ion-gel electrolyte mimics the synaptic cleft. Presynaptic gate voltage spike induces migration of mobile anions near the ONW surface, which corresponds to the postsynaptic membrane. The accumulated anions attract holes to the ONW; they increase the excitatory postsynaptic current (EPSC) that flows between source and drain electrodes. When a single short spike voltage is applied, a sharp EPSC peak is triggered, which decays to a resting current. If several spikes are applied in quick succession, ions accumulate near the surface of ONW, so EPSC increases gradually. After spikes, accumulated anions spread back and become dispersed randomly in the electrolyte; as a result, the original resting current is restored.

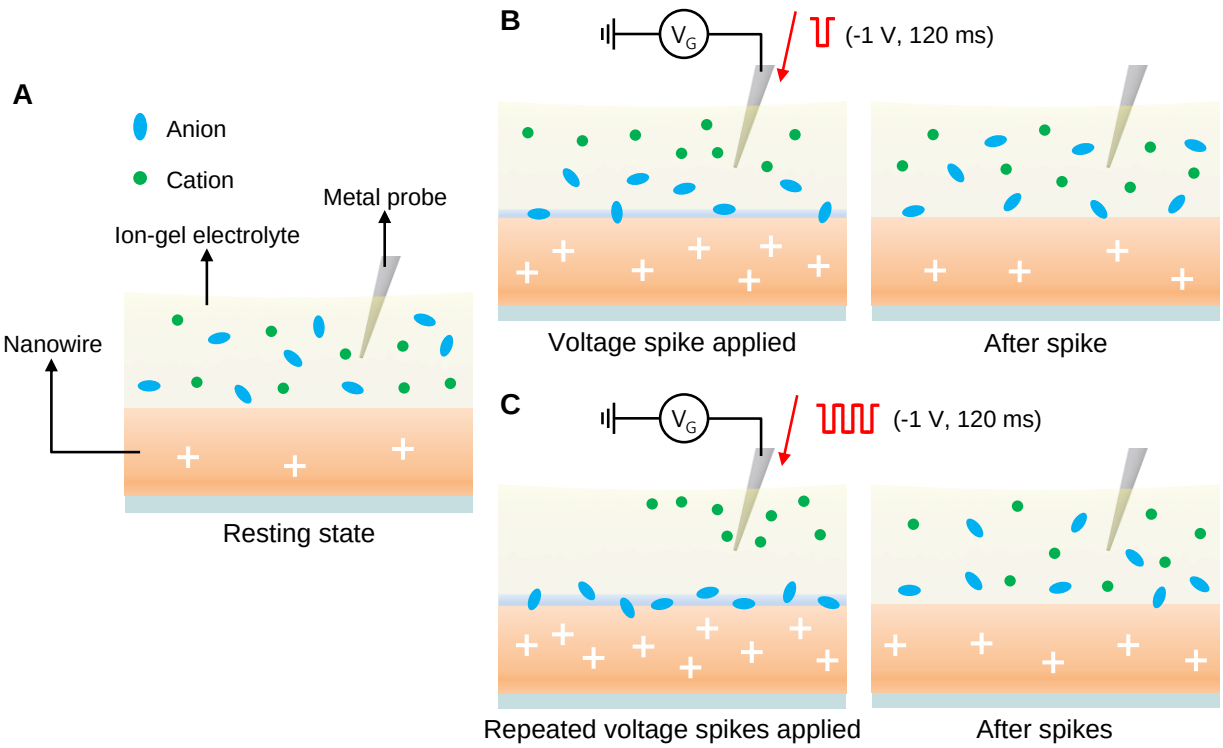

Fig. S1. Working mechanism of s-ONWST. (**A**) During the resting stage, anions and cations are randomly distributed in ion-gel electrolyte. (**B**) With a gate voltage spike, a few anions migrate to near the surface of the ONW and induce holes in ONW temporally, so a brief EPSC develops. After the spike, ions diffuse back to the original equilibrium state and the current decays to the resting state. (**C**) With repeated gate voltage spikes, an increasing number of anions accumulate near the surface of the ONW and attract holes in the ONW, so EPSC increases. Some anions may migrate a short distance into the ONW. After spikes, ions diffuse back to the equilibrium state and the current decays to the resting state.

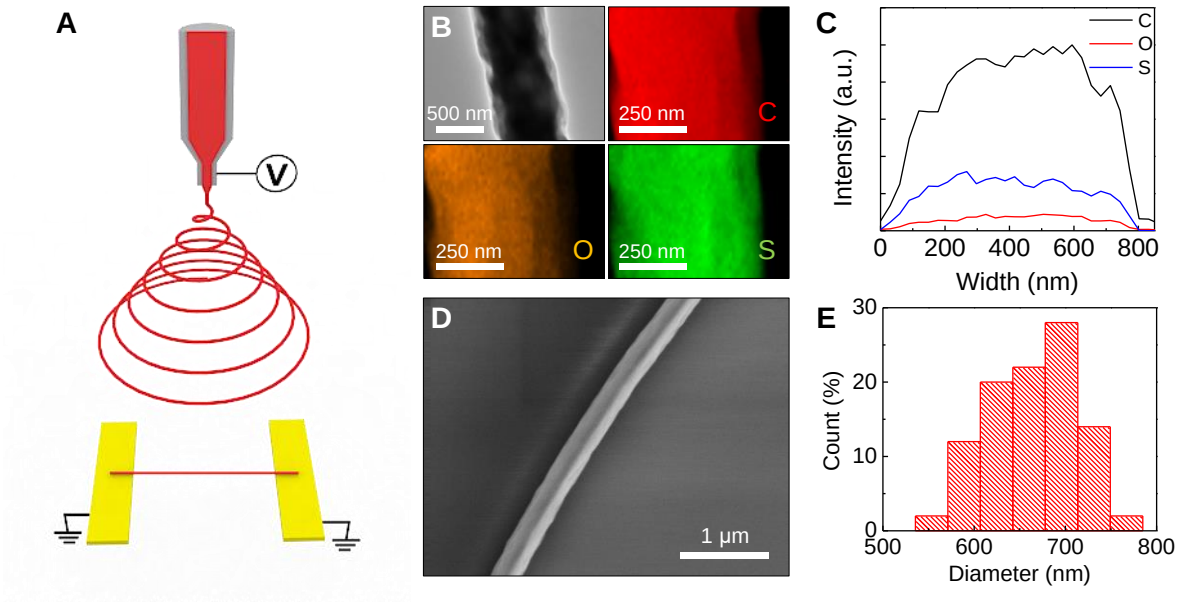

Fig. S2. Fabrication and morphology of ONW. (**A**) Electrospinning of an aligned single ONW using parallel electrodes. (**B**) Transmission electron microscopy image and energy-dispersive X-ray spectroscopy mapping of ONW (red: carbon, orange: oxygen, green: sulfur). (**C**) Line profile for chemical elements of ONW (black: carbon, red: oxygen, blue: sulfur). ONW has homogenous chemical composition. (**D**) Scanning electron microscopy image of ONW. (**E**) Diameter distribution of ONW. Average diameter was 664 (s.d. 47) nm.

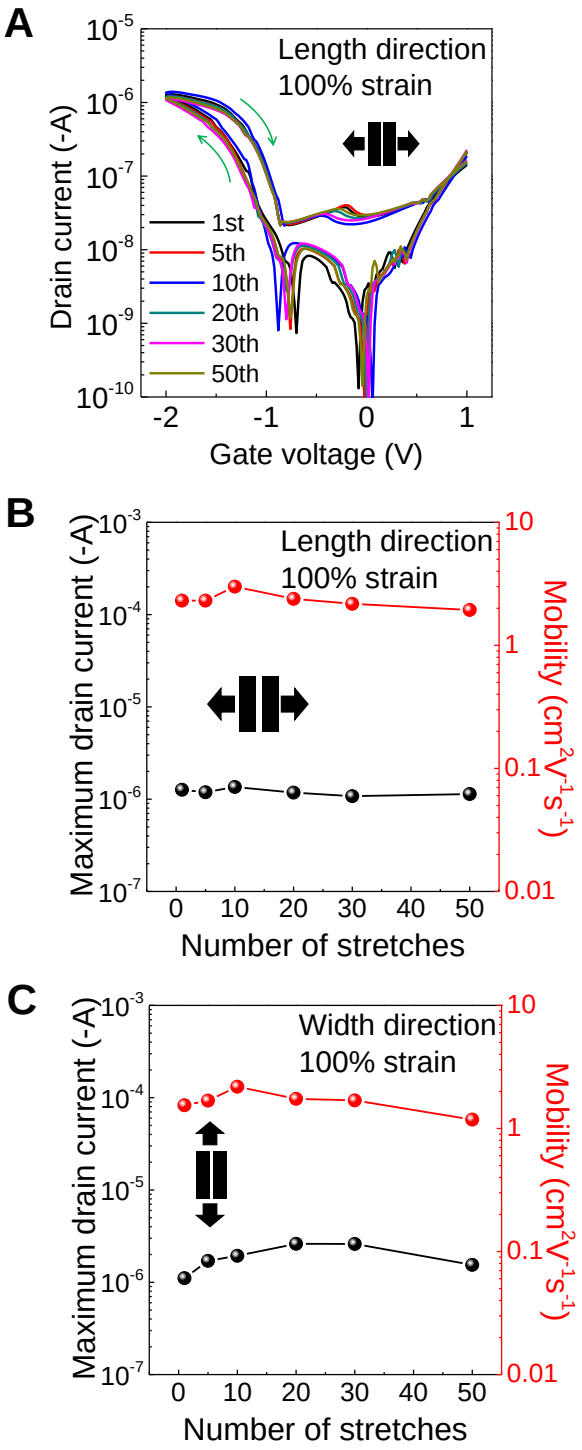

Fig. S3. Electrical characteristics of s-ONWST. (**A**) *I-V* characteristics of s-ONWST after stretching cycles at 100% strain. Blue arrows: clockwise hysteresis. (**B** and **C**) Maximum drain current and mobility after stretching cycles at 100% strain along the channel (B) length and (C) width directions.

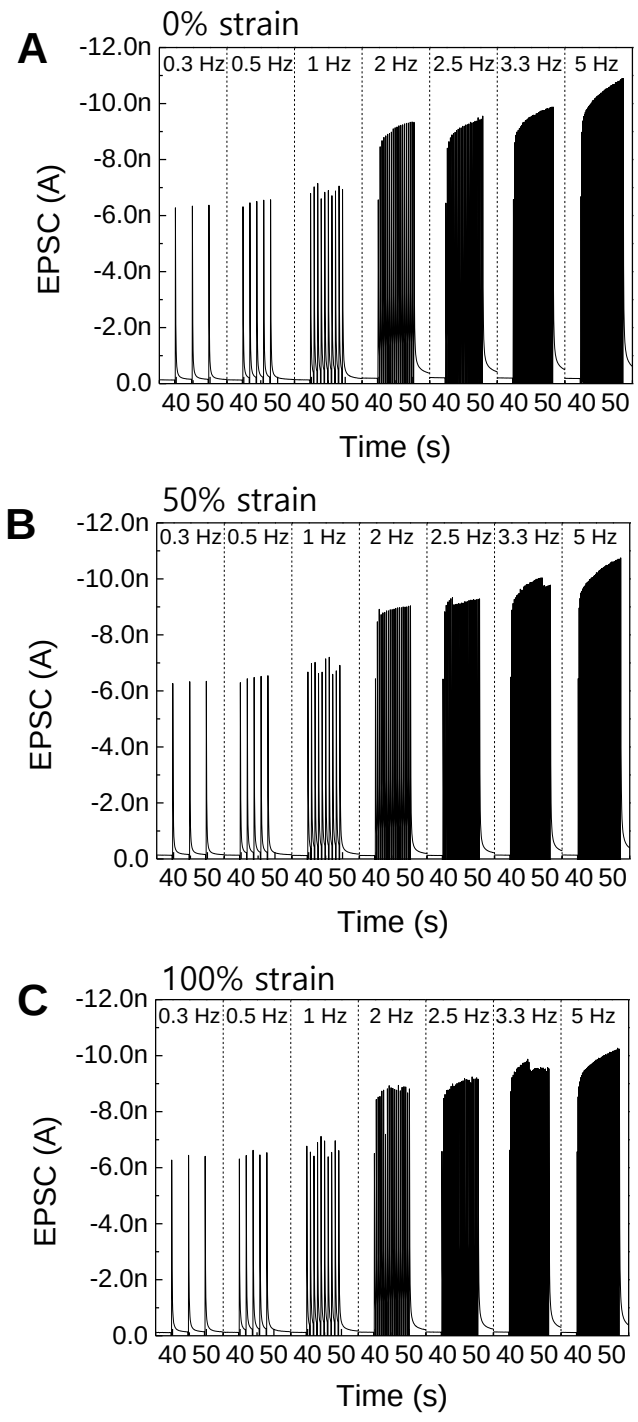

Fig. S4. SFDP of s-ONWST. (**A-C**) EPSCs of artificial synapse with spike frequency from 0.3 to 5 Hz at (A) 0% strain, (B) 50% strain and (C) 100% strain.

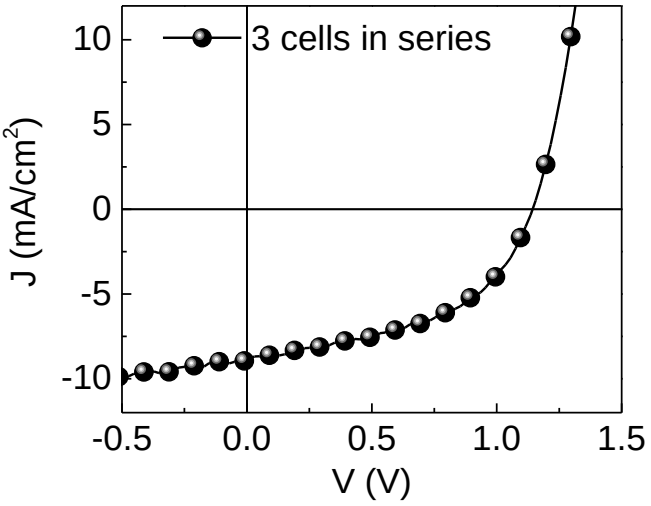

Fig. S5. Current density-voltage (*J*-*V*) characteristics of organic photodetector. Three sub-pixels (total area ~ 0.48 cm^2) were connected in series and generated V_{OC} = -1.1 V.

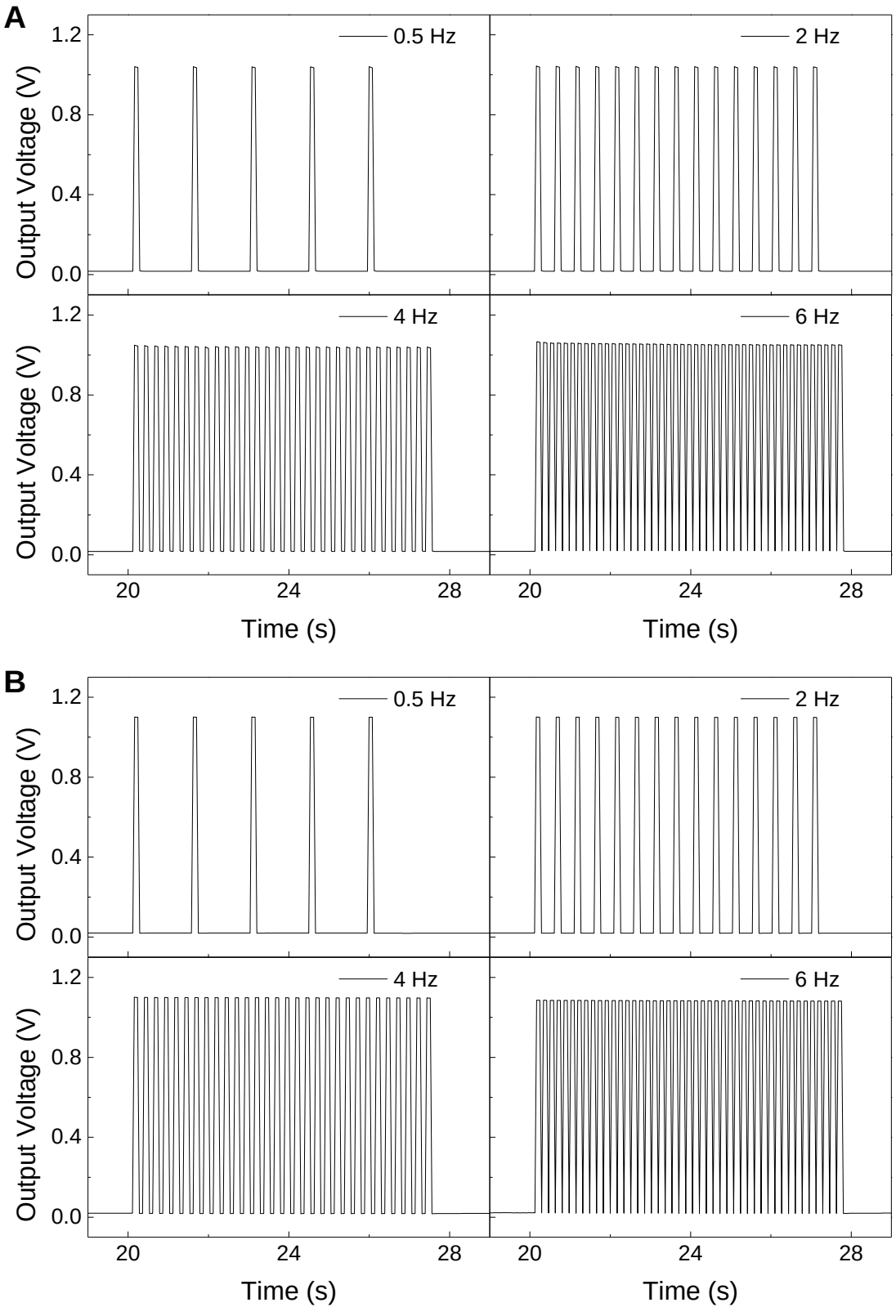

Fig. S6. Output characteristics of the photodetectors with different light spike frequency. Output voltage of (A) the organic photodetector and (B) the silicon photodetector with light-spike frequency from 0.5 to 6 Hz.

Muscle contraction and EPSCs of s-ONWST

According to the number and frequency of action potentials, skeletal muscle is activated in four ways: twitch, summation, incomplete tetanus, and complete tetanus. A twitch is a small contraction and relaxation; the combination is induced by a single impulse, and is similar to a single EPSC in an s-ONWST. If two impulses arrive within short interval, muscle contraction increases because the second contraction is added before the first contraction is completely released; this condition is similar to the paired-pulse facilitations in an s-ONWST. As the number of impulses increases, muscle contractions increase; this is incomplete tetanus and is analogous to the gradual increase of EPSCs in an s-ONWST. When action potentials occur very frequently, consecutive twitches fuse; the result is continuous muscle contraction, which is complete tetanus. When an s-ONWST is stimulated with small interspike interval Δt in the same period, EPSCs increased almost linearly then saturated; this response curve resembles tetanus (fig. S7). Therefore, organic neuromuscular electronic system emulates a biological neuromuscular system well.

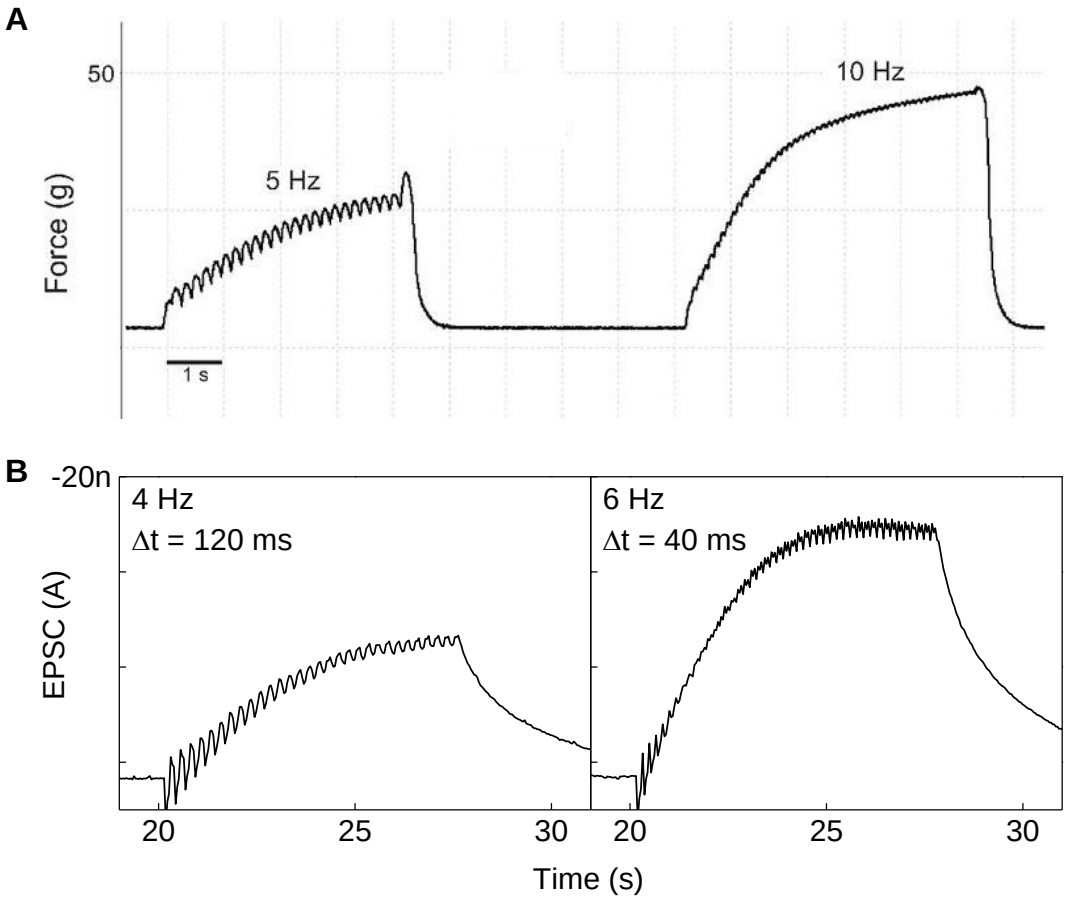

Fig. S7. Frequency-dependent biological muscle contraction and EPSCs of s-ONWST. (**A**) Recording of force-frequency of a soleus muscle of a rat (*32*). Reproduced with permission. Mechanical summation and incomplete tetanus with stimulus frequency f_{SPIKE} = 5 Hz and fused tetanus with f_{SPIKE} = 10 Hz. (**B**) EPSCs of s-ONWST with f_{SPIKE} = 4 Hz (with interspike interval Δt = 120 ms) and 6 Hz (with Δt = 40 ms) which are similar to f_{SPIKE}-dependent muscle contraction.

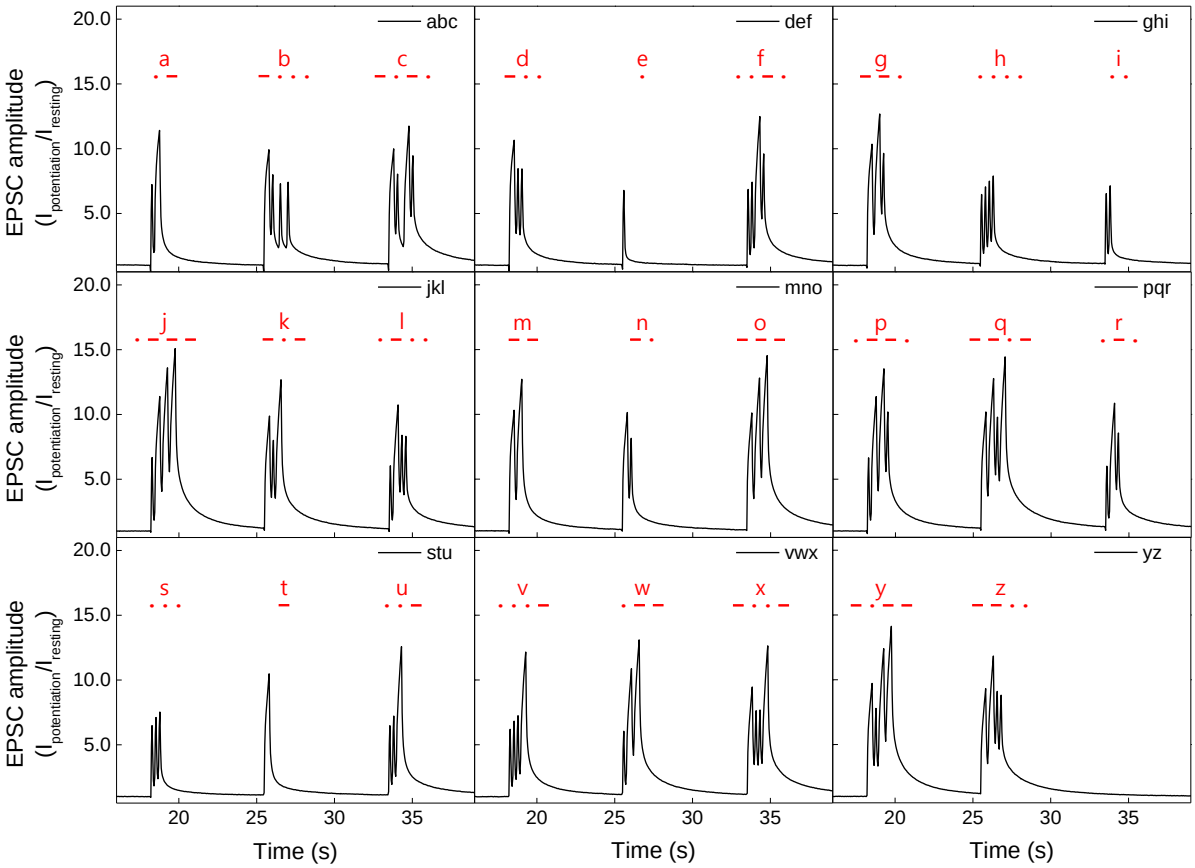

Fig. S8. A novel optical wireless communication method of human-machine interface. Visible light-triggered EPSC amplitude of s-ONWST with International Morse code. Every letter produces a distinct EPSC amplitude response.

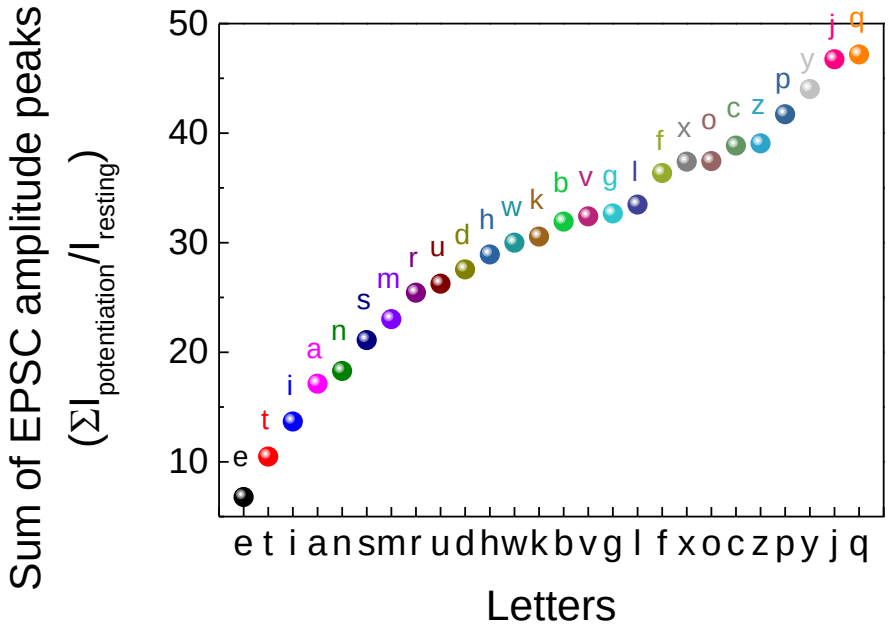

Fig. S9. Correlation between EPSC amplitude response and the International Morse code of English letters. Every letter was linearly correlated with the sum of EPSC amplitude peak values.

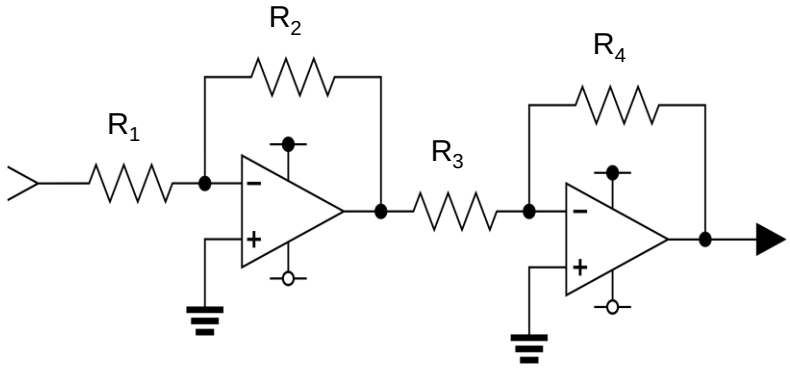

Fig. S10. Full circuit diagram of transimpedance circuit. The circuit was developed on a breadboard with R_1 (1 MΩ), R_2 (10 MΩ), R_3 (1 kΩ), R_4 (10 kΩ) and two dual-supply operational amplifiers (CA3130, Intersil corporation).

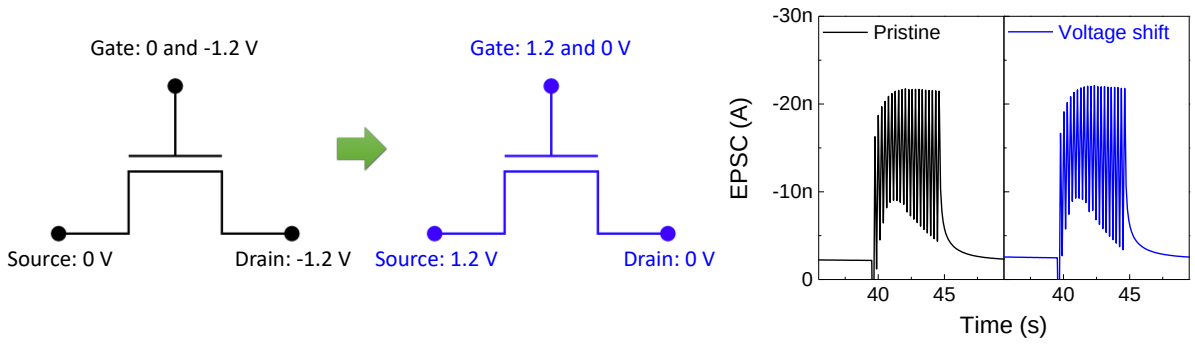

Fig. S11. Operating voltage shift of s-ONWST to connect the transimpedance circuit. Pristine applied voltage for each source and drain electrode of s-ONWST is 0 and -1.2 V, and gate voltages are 0 V for resting state and -1.2 V for spike. To operate the polymer actuator, the drain electrode was connected to the trans-impedance circuit, so this electrode could not apply the drain voltage. Therefore the applied voltage for each electrode was shifted while maintaining overall potential (source voltage: 1.2 V, drain voltage: 0 V, gate voltage: 1.2 V for resting state and 0 V for spike). The pristine and shifted operating condition generated almost the same EPSC characteristics.

Table S1. Summary of electrical characteristics of s-ONWST as function of strain in channel length and width directions.

Strain (%)	Length direction		Width direction	
	Maximum drain current (-μA)	Mobility ($cm^2 \cdot V^{-1} \cdot s^{-1}$)	Maximum drain current (-μA)	Mobility ($cm^2 \cdot V^{-1} \cdot s^{-1}$)
0	1.50	3.54	1.19	1.58
25	1.37	3.00	1.00	1.79
50	1.60	2.93	0.83	1.62
75	1.62	2.50	1.57	1.61
100	1.68	2.86	1.58	1.32

Table S2. Summary of electrical characteristics of s-ONWST after stretching cycles at 100% strain in channel length and width directions.

Number of stretches	Length direction		Width direction	
	Maximum drain current (-μA)	Mobility ($cm^2 \cdot V^{-1} \cdot s^{-1}$)	Maximum drain current (-μA)	Mobility ($cm^2 \cdot V^{-1} \cdot s^{-1}$)
1	1.26	2.31	1.11	1.54
5	1.19	2.31	1.71	1.68
10	1.36	3.00	1.93	2.18
20	1.18	2.39	2.61	1.74
30	1.08	2.18	2.60	1.69
50	1.14	1.94	1.54	1.18

Table S3. Maximum δ of polymer actuator and output voltage generated by s-ONWST according to the number of light spikes.

Number of spikes	Displacement (mm)	Output voltage (V)
0	0.39	~ 1[a]
10	1.50	1.33
30	2.06	1.96
50	2.50	2.68
60	2.72	3.20

[a]Output voltage converted from resting current without light spike

Movie S1. Operation of an artificial muscle actuator by an optical sensory neuromuscular electronic system.